



## Short communication

# A one-tube multiplexed colorimetric strategy based on plasmonic nanoparticles combined with non-negative matrix factorization



Yizhen Liu<sup>a</sup>, Wei Fang<sup>a</sup>, Zitong Wu<sup>a</sup>, Guohua Zhou<sup>a</sup>, Wen Yi<sup>b</sup>, Xiaodong Zhou<sup>a</sup>, Aiguo Shen<sup>a</sup>, Jiming Hu<sup>a,\*</sup>

<sup>a</sup> Key Laboratory of Analytical Chemistry for Biology and Medicine (Ministry of Education), College of Chemistry & Molecular Sciences, Wuhan University, Wuhan 430072, China

<sup>b</sup> School of Naval Architecture & Ocean Engineering, Huazhong University of Science and Technology, Wuhan 430072, China

## ARTICLE INFO

## Article history:

Received 20 January 2014

Received in revised form

8 April 2014

Accepted 9 April 2014

Available online 30 April 2014

## Keywords:

Detection

Colorimetry

Oligonucleotides

Nanoparticles

Non-negative matrix factorization

## ABSTRACT

Herein, a one-tube colorimetric platform has been developed for the simultaneous determination of two analytes (DNA as model object) in one tube with picomolar sensitivity. SPR-active nanoparticles are used to encode reporter probes sensitive to oligonucleotides associated with hepatitis A virus V<sub>all7</sub> polyprotein gene (HVA) and hepatitis B virus surface-antigen gene (HVB) respectively and magnetic beads (MBs) serve as the removal tool. In this mixed nanoparticles based biosensor, the addition of target analytes could change the concentration of each nanoparticle, leading to different colors of the supernatant. The influence of spectral overlap has been eliminated by a non-negative matrix factorization (NMF). With the assistance of NMF, the limit of detection (LOD) can be determined as pM level without amplification. On the whole, this nanosensor boasts the advantages of high sensitivity and low sample consumption. Simultaneous colorimetric detection and quantification of two molecules in one tube are demonstrated.

© 2014 Elsevier B.V. All rights reserved.

## 1. Introduction

There has been an ever-increasing need to develop highly sensitive and selective methods in various fields including molecular diagnostics and bioterrorism [1–3]. A particularly attractive material toward this aim is plasmonic noble metal nanoparticle. Gold nanoparticles (GNPs) is one of the typical choices that features high extinction coefficient, unique optical property and mature surface functionalization methods [4–6]. By adding the target molecules simultaneously bound to the two sets of oligonucleotide-modified GNPs, particle aggregation can be achieved by the formation of the sandwich hybridization structure of GNPs-target-GNPs [4]. With naked-eye observation, the color of the colloid takes an obvious change from red to purple just like the litmus which is caused by the red shift of the surface plasmon peak. Numerous colorimetric methods based on the color change in the aggregation of metal nanoparticles have been developed and applied to the detection of DNA [4,7], protein [8], ions [9] and small molecules [10,11].

Since their original design, GNPs have been refined in various aspects. The choice of probes is of particular interest as it may lead to simpler spectra readout and further fit to multiplex detection. Multiplexed analysis which is reasonable and high-throughput, has been identified as an important detection method since it is able to screen multiple analytes in a single assay, being rapid, simple and consumes fewer samples and reagents [9,12–14]. One of the fundamental ways is using more probes such as silver nanostructures [15,16]. However, the ability to quantify targets is largely determined by the overlap of the spectra [17]. Furthermore, while quantitative colorimetric detection has been developed for several years, most of the previous works only use the peak intensity or relative intensity between dispersed/aggregated GNPs [18,19]. Therefore, the real challenge in the multiplexed method is the development of a proper quantification indicator. Notably, although traditional GNPs have proven effective to response the existence of target molecules, methods using magnetic beads (MBs) combined with GNPs can reduce the particle sedimentation and the complexity of spectra [20].

Herein, we design a strategy that can give a fast signal response of targets by a simple mixing of sensors for simultaneous multiplex analytes detection in one tube. The colorimetry using non-aggregated GNPs combined with MBs shows high sensitivity and selectivity [20], which features unique advantages over traditional

\* Corresponding author. Tel.: +86 027 68752439.

E-mail address: [jmhu@whu.edu.cn](mailto:jmhu@whu.edu.cn) (J. Hu).

colorimetric assays and could be improved for further application by using other noble metal nanoparticles. As silver core–shell nanoparticles (SNPs) show similar detection capability with GNPs [17], yet rather different optical signals, we employ SNPs together with GNPs in the non-aggregation based colorimetric system for multiplex detection of analytes. To prevent ambiguities related to color determination by naked-eye analysis of the assay, a fully functional NMF-based data analysis was developed for quantitative determination of a DNA mixture. We believe that the combination of non-aggregated nanoparticle-based colorimetric methods and NMF analysis can be potentially used in the multiplexed determination of biomolecules. Based on this finding, for the first time we demonstrate the feasibility of using non-aggregated metal nanoparticles colorimetry in the simultaneous detection of multiple targets.

## 2. Experimental

### 2.1. Materials

All reagents were purchased from Sinopharm Chemical Reagent Co. Ltd. with analytical reagent grade and used without further purification. Ultrapure water was used throughout the experiments. Carboxyl-coated magnetic beads (1.05  $\mu\text{m}$  Dynabeads<sup>®</sup> MyOne<sup>™</sup>, 10 mg mL<sup>-1</sup>) were purchased from Invitrogen Dynal<sup>®</sup> AS. PB solution (10 mM phosphate sodium buffer solution, pH 7.4), PBS-T buffer (10 mM phosphate sodium buffer solution, pH 7.4, 100 mM NaCl, 0.05% tween-20), MES buffer (2-[N-morpholino]ethane sulfonic acid, 100 mM, pH 4.8), and Tris buffer (2-amino-2-hydroxy-methyl-1,3-propanediol, 50 mM, pH 8).

The sequences of two capture probes were as follows:

- Capture probe HVA (CHVA), 5' NH<sub>2</sub>-AAAAAAAAAAGAAAGAG-GAGTTAA-3',
- Capture probe HVB (CHVB), 5' NH<sub>2</sub>-AAAAAAAAATACCACAT-CATCCAT-3'.

The sequences of reporter probes were as follows:

- Reporter probe HVA (RHVA), 5'-TCCATGCAACTC-TAAAAAAAAAAAA-SH 3',
- Reporter probe HVB (RHVB), 5'-ATAACTGAAAGC-CAAAAAAAAAAAAA-SH 3'

The two target oligonucleotides were as follows:

- target HVA, 5'-TTAGAGTTGCATGGATTAACCTCTTTCT-3',
- target HVB, 5'-TTGGCTTTCAGTTATATGGATGATGTGGTA-3'.

Each reporter and capture sequence had a A10 as the linker for better hybridization. All above oligonucleotides were purified by HPLC and synthesized by Shanghai Sangon Biological Engineering Technology & Services Co.

### 2.2. Equipment

UV–vis absorption spectrometer: UV-2550 (Shimadzu). Centrifuge: TG16W (Changsha Pingfan Instruments & Meters Co. Ltd.). Shaker vortex: Genius 3 (IKA Works, Inc.).

### 2.3. Preparation of probes

Citrate-stabilized GNPs were prepared by thermal reduction of HAuCl<sub>4</sub> with sodium citrate. SNPs were prepared by a seed-mediated method similar with the previous report [21]. 1.05  $\mu\text{m}$

Dynabeads<sup>®</sup> MyOne<sup>™</sup> carboxyl-coated magnetic beads were purchased from Invitrogen Dynal<sup>®</sup> AS.

We designed two MBs modified capture probes, one GNPs and one SNPs labeled reporter probe, and two target oligonucleotides which were associated with hepatitis A virus Vall7 polyprotein gene (HVA) and hepatitis B virus surface-antigen gene (HVB), as models to demonstrate the multi-color nanosensor for multiple DNA detection. Each target oligonucleotide was complementary to one capture probe and one GNPs or SNPs labeled reporter probe in a sandwich structure.

The optical nanoprobe we prepared were with sulphydryl oligonucleotides (reporter probe) on the surface of GNPs and SNPs, and with amino oligonucleotides (capture probe) modified on the surface of MBs. The reporter probes were covalently linked to metal nanoparticles for use as the signal source using the method similar to those previously described [22]. Amino capture probe was covalently linked to carboxylated MBs for use as the capture tool by the (N-Ethyl-N'-(3-dimethylaminopropyl) carbodiimide hydrochloride (EDC) crosslink reaction, following the protocol suggested by the manufacturer. The hybridization was performed in a buffer solution containing 10 mM phosphate sodium, 100 mM NaCl, 0.05% tween-20, pH 7.4.

### 2.4. Protocol of the two-color colorimetry

In a typical non-aggregated nanoprobe-based DNA detection experiment, 1  $\mu\text{L}$  sample solution containing target DNA in the single-stranded form was added to an appropriate amount of MBs probes (10 mg mL<sup>-1</sup>, PBS-T buffer) solution to initiate the assay. The GNPs probes (35  $\mu\text{L}$ , PBS-T buffer) and the SNPs probes (35  $\mu\text{L}$ , PBS-T buffer) were then added to the solution and allowed to hybridize with a gentle vortex for 90 min. The total volume was increased to 80  $\mu\text{L}$  with PBS-T. After hybridization, the MBs with target-linked SNPs/GNPs together with unreacted MBs were easily pulled to the wall of the tube in about one minute by applying an external magnetic field. After the separation, the supernatant was tested by a Shimadzu UV-2550 with a 50  $\mu\text{L}$  quartz micro-cuvette. The whole process was carried out at room temperature 25 °C.

### 2.5. Non-negative matrix factorization analysis

NMF based on “multiplicative” iteration rules is a multi-variant analyzing method using non-negative constrains to generate the approximate data which can be applied in an analytical field [23,24]. Given an initial non-negative matrix ( $V$ ), it is possible to find two non-negative matrices, the basis matrix ( $W$ ) and coefficient matrix ( $H$ ) to approximate the original matrix. In the processing of the data for this experiment, all UV–vis spectra were combined to form matrix  $V$  (Fig. 1). The number of factors was set as 2 for there are two kinds of nanoparticles in the supernatant. Low-rank matrices  $W$  and  $H$  were automatically started from random matrices and stopped when matrix has not changed for 10,000 iterations. Matrix  $W$  corresponds with the basic spectra for pure SNPs and GNPs and  $H$  corresponds to the intensity coefficient.

UV–vis spectroscopic data were exported from the instrument software into MATLAB (The Math-Works, Inc., Natick, MA) where NMF data processing was performed in order to allow direct quantification of the targets.

## 3. Results and discussion

### 3.1. Principle of two-color colorimetry for two analytes detection

The basic design of this two-color colorimetric nanosensor is shown in Fig. 2. Two metal nanoparticles labeled reporter probes,

and two MBs modified capture probes were employed. Firstly, two kinds of oligonucleotide probes, RHVA and CHVA, were used to recognize the oligonucleotide related to hepatitis A virus (HVA). Similarly, RHVB and CHVB were designed to detect the target oligonucleotide hepatitis B virus (HVB). To establish the multiplexed detection system for DNA, the original mixtures containing RHVA, CHVA, RHVB, and CHVB were prepared, and then samples containing the target DNA were added in to form the sandwich structure. After the hybridization, a magnet was used during the removal process, and the unbound metal nanoparticle remain dispersed in the supernatant. Further, the information of color varied according to the ratio of two target DNAs introduced to the sensor. This interesting color effect is useful in the simultaneous detection of two target DNAs in one tube. One obvious advantage of this strategy was that it avoided the aggregation between optical nanoparticles, which further avoided the sedimentation. As this strategy only affected the intensity of the extinction peak instead of the peak position, the information of spectra featured an inherent simplicity for quantification.

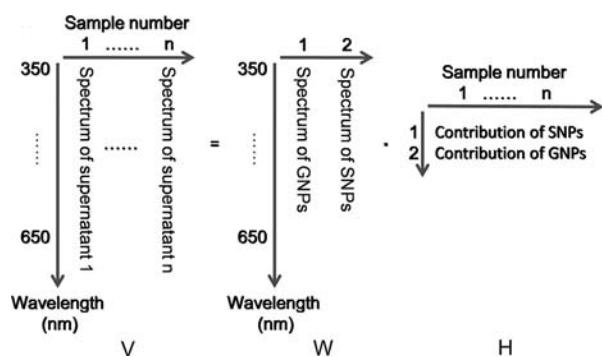


Fig. 1. The principle of NMF analysis that processes the UV-vis spectra.

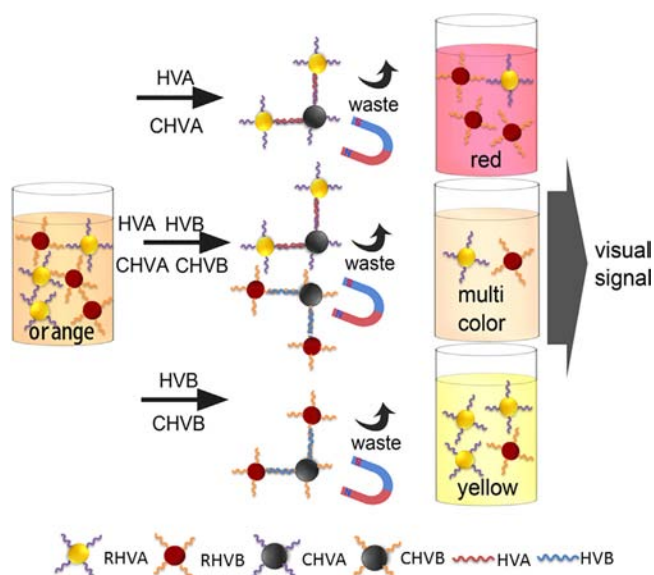


Fig. 2. Schematic illustration of non-aggregated nanoparticles based two-color colorimetric biosensor for DNA detection. The RHVA and RHVB are originally mixed and show a color of orange, but the color will change after incubation with the target DNA due to the reduction of reporter probes. As the increase of target DNA, the color of solution change significantly from orange to red or yellow. (For interpretation of the references to color in this figure, the reader is referred to the web version of this article.)

### 3.2. Optimization of variables

The reaction time of nanosensors is a significant parameter for the evaluation of colorimetric approach. Analytes were added at the time point of 0 s, and spectra changes were observed. The maximum absorption value change of HVA or HVB (Fig. S1) were recorded after addition of HVA or HVB and the incubation were maintained at 25 °C for 90 min. It should be noted that the optimization of this aspect was not carefully investigated. However, a variety of factors can affect the hybridization of GNPs and MBs which include the size of the nanoparticles, salt concentration and the surface density of the oligonucleotides on the nanoparticles [25]. Therefore, it is possible to shorten the reaction time by increasing the salinity which is consistent with the electrostatic interactions (repulsion between GNPs and MBs), or lowering the surface coverage of oligonucleotides, as reported by literatures [26,27].

Sensitivity of colorimetric approach in the presence of varying amounts of MBs was also monitored. The best working concentration of the MBs were determined with unchanged concentration of optical probes and target DNA. The results in Fig. S2 have shown that the parameters for SNPs and GNPs to achieve its highest sensitivity are different. This difference is largely due to the difference in the amount of DNA modified on the surface of each particle and the distinct extinction coefficient of the particles. The amount of modified DNA on the surface of nanoparticle has an inverse relationship with its sensitivity [20]. In addition, even with the same modifying and maturing method, the density of DNA on the surface of SNPs and GNPs are different. These differences have led to different optimal amounts of MBs needed for different particles to be combined with MBs in the colorimetry based on non-aggregated particles.

### 3.3. Detection of sequences at single-target model

To investigate the feasibility of the strategy, we firstly tested the single-target model. With an external magnetic field, SNPs that were bound to magnetic beads through target-induced hybridization were removed from the mixed solution. As a result, the absorption intensity of SNPs reduced and the GNPs signal was denoted as a background signal, and visually the color of supernatant changed from orange to red. The appearance of such signals indicated the presence of target DNA HVA in the sample (Fig. 3). No signal change could be observed in the absence of target DNA HVA, due to that SNPs could not be cross-linked to the MBs. Similarly, in the presence of target DNA HVB, only GNPs were able to hybrid with CHVB to form a sandwich complex through DNA assembly. After the removal operation, the color of supernatant appeared closer to yellow compared with the original color, which indicated the existence of target HVB. Hence, the change of supernatant in color by DNA targets proved the selectivity of the design and feasibility of the principle as a two-color biosensor. The intensity of 430 nm peaks assigned to SPR extinction of SNPs decreased obviously with addition of the HVA target. Fig. 3 has shown the linear fit data of signal changes of supernatant as a function of the concentrations of target HVA. The linear range of HVA was from 10 to 125 pM under a simple optimal conditions of the amount of MBs. In a similar way, as the HVB DNA concentration increased, the intensity of 530 nm peak from GNPs decreased noticeably, which resulted in the color change of the supernatant from orange to yellow. The UV-vis spectra information showed a linear change over the range of 25–175 pM. Therefore, the signal of supernatant changed linearly with the addition of targets. The results confirmed the applicability of the single-target biosensor and the feasibility of the principle that the target DNA can be

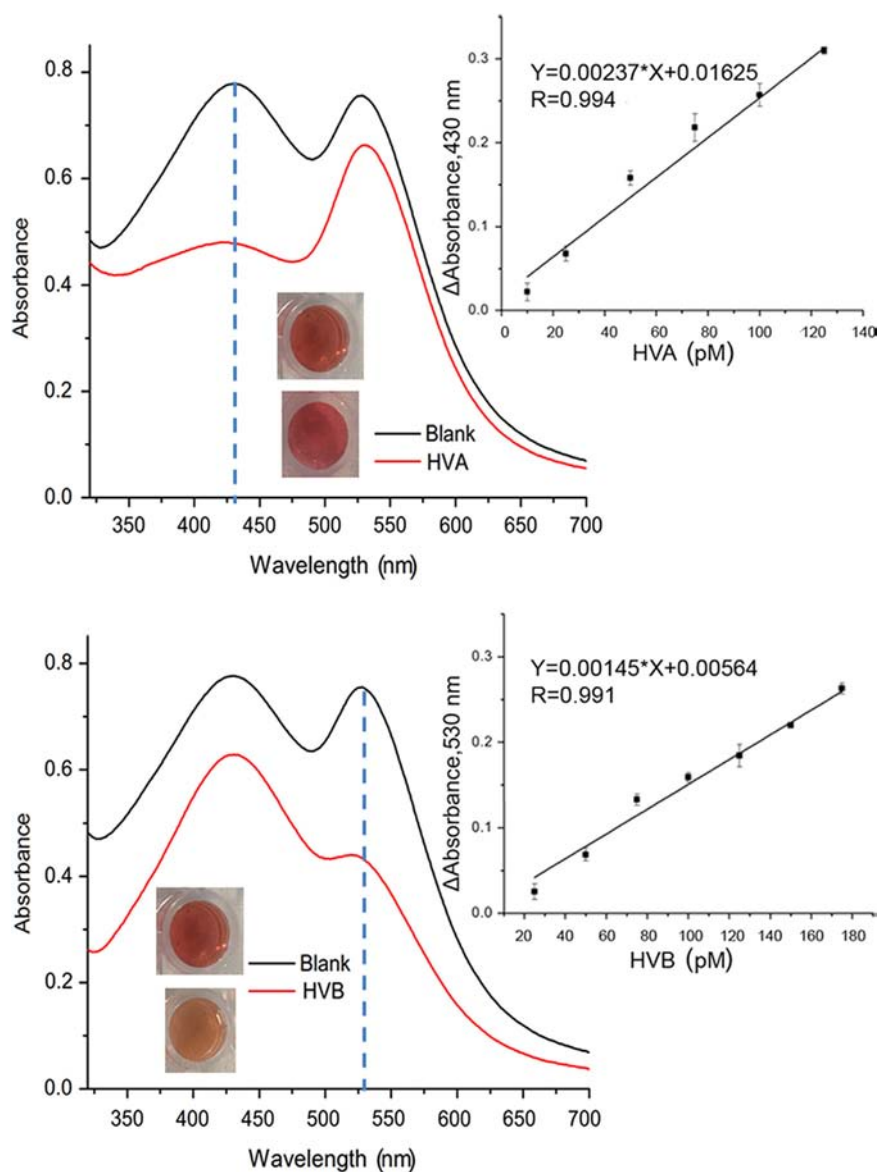


Fig. 3. UV-vis spectra, digital images and fit linear data of the HVA sensor and the HVB sensor.

respectively hybridized with the probes so that the relative metal nanoparticle would be magnetically eliminated.

#### 3.4. Simultaneous determination of two DNA in one tube

Simultaneous determination of different DNAs in one tube was then investigated and performed through the non-aggregated based two-color strategy. As there exists two directions of color conversion (orange to red or yellow) in our methods, it is attractive to run only one test for one-tube recognition of two targets which features less sample and time consuming. We evaluated the performance of a two-color nanosensor to investigate the practical applicability of our strategy for one-tube determination of multiple DNA. A  $6 \times 6$  matrix was built in a microplate, in which each element was a sample containing different concentrations of HVA and HVB. Interestingly, the color change was significantly different, and varied from 10 to 125 pM for HVA and 25 to 150 pM for HVB. Fig. 4 shows a photograph displaying the color change of these DNAs using one 96-well microplate. The performance of the two-color mode was evaluated by UV-vis measurements in the same way. As shown in Fig. 4, both the SPR absorption peaks decreased

simultaneously when a sample solution containing both HVA and HVB was added. However, the spectra cannot be analyzed as easily as the visual signals due to the overlap and interference between UV-vis spectra of SNPs and GNPs. One important aspect that leads to such interference was that the spectra of SPR-active nanoparticles were not narrow enough to eliminate the overlap, which successively disturbed the quantification. In order to clearly analyzed the spectra and quantify the two DNA targets, we firstly introduce NMF to factorize the series of experimental data into two basic data groups in need.

#### 3.5. Non-negative matrix factorization and quantitative analysis.

It indicated that the concentrations of the respective nanoparticles were determined by the concentrations of the two kinds of DNA. Therefore, the simultaneous quantitative analysis of DNA would be possible by measuring the absorbance of these two kinds of metal nanoparticles relating to the DNA targets. By conduction of NMF analysis, we established a one-tube quantitative determination for two analytes that works even when it is difficult to quantify the targets in a complex sample due to the overlap of the

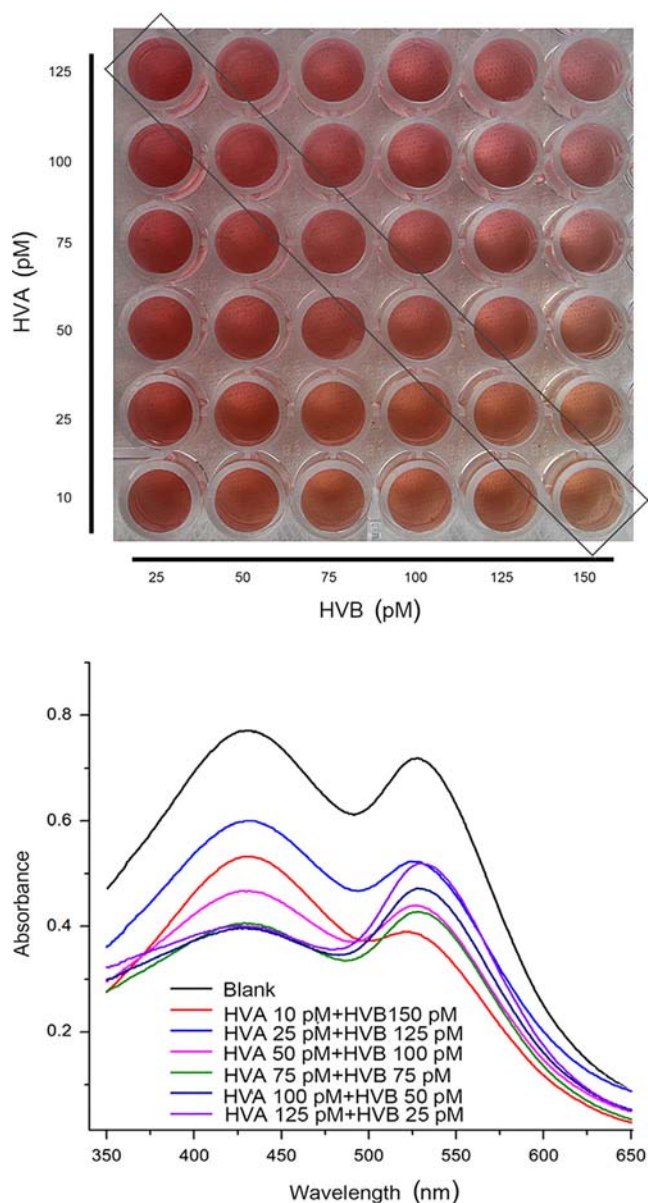
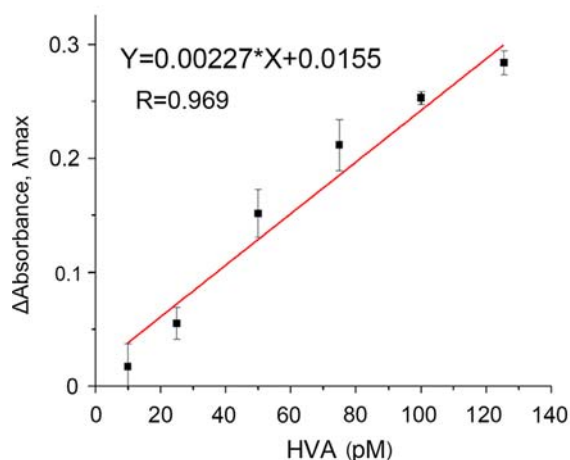


**Fig. 4.** Photograph displaying the color change of the supernatant after incubation at 25 °C for 90 min with the presence of different concentrations of HVA and HVB mixtures. UV-vis spectra of supernatant with different concentrations of targets in the rectangular area of the photograph.



two spectra. The target concentrations were quantified by analyzing the changes in the absorption intensity acquired through NMF, and the interference of the overlap between different SPR-active nanoparticles can be solved automatically with this method. The multivariate evaluation schemes introduced in this essay can reduce the interference of spectral overlap on the scale of the entire UV-vis spectrum rather than just a single peak as in their univariate counterparts [24]. Using the relative intensities of maximum absorbance peak of SNPs and GNPs acquired from NMF, the results clearly show the real intensities of optical probes instead of the overlapping spectra. Fig. 5 shows the quantitative result of the multiple target DNA detection with two-color colorimetry, which is almost identical with Fig. 3. The result verified the validity of the NMF method. The data before and after the NMF process echoed with each other and confirmed that the linear analysis remains undisturbed. According to the data in Fig. 5, the LOD of HVA was 9 pM as calculated, whereas the LOD of HVB was 15 pM, which proved the high sensitivity of the method.

#### 4. Conclusions

In conclusion, we have demonstrated a two-kind non-aggregated metal nanoparticles based two-color colorimetric method for two analytes detection. In this two-color nanosensor, the information of supernatant were used as signals. Our approach has significant advantages of low cost, high sensitivity and high selectivity. Combined with an automatic NMF chemometrics analysis, this colorimetry offers a simple and quantifiable route for multiple analytes detection in one tube with detection limits of 9 pM for HVA and 15 pM for HVB. Using noble metal nanoparticles with unique SPR properties such as Ag and Pt as signal sources, this novel platform has great potential to be used for the simultaneous multiplexed detection of proteins, ions and small molecules. Furthermore, because this two-color colorimetric method takes advantage of a simple “seeing is believing” assay, it might have potential to be an android-based color analysis system [28], and have practical applications in clinical diagnostics.

#### Acknowledgment

We gratefully acknowledge the support from the National Natural Science Foundation of China (NSFC) (Nos. 20927003, 90913013, 41273093 and 21175101), National Major Scientific Instruments and

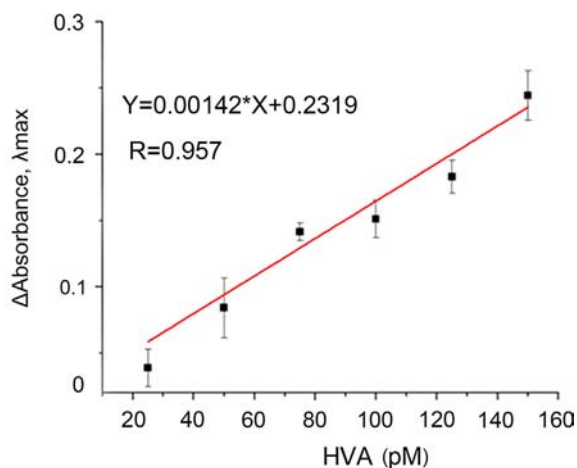


**Fig. 5.** Linear fit data of the supernatant towards different concentrations of HVA and HVB in one tube.

Device Development Project (2012YQ16000701), and Foundation of China Geological Survey (Grant no. 12120113015200).

## Appendix A. Supplementary material

Supplementary data associated with this article can be found in the online version at <http://dx.doi.org/10.1016/j.talanta.2014.04.051>.

## References

- [1] S. Song, Y. Qin, Y. He, Q. Huang, C. Fan, H.-Y. Chen, *Chem. Soc. Rev.* 39 (2010) 4234–4243.
- [2] D.A. Giljohann, C.A. Mirkin, *Nature* 462 (2009) 461–464.
- [3] P.D. Howes, S. Rana, M.M. Stevens, *Chem. Soc. Rev.* (2014).
- [4] R. Elghanian, J.J. Storhoff, R.C. Mucic, R.L. Letsinger, C.A. Mirkin, *Science* 277 (1997) 1078–1081.
- [5] H. Jans, Q. Huo, *Chem. Soc. Rev.* 41 (2012) 2849–2866.
- [6] R.A. Sperling, P. Rivera Gil, F. Zhang, M. Zanella, W.J. Parak, *Chem. Soc. Rev.* 37 (2008) 1896–1908.
- [7] J.J. Storhoff, R. Elghanian, R.C. Mucic, C.A. Mirkin, R.L. Letsinger, *J. Am. Chem. Soc.* 120 (1998) 1959–1964.
- [8] X. Xu, M.S. Han, C.A. Mirkin, *Angew. Chem. Int. Ed.* 46 (2007) 3468–3470.
- [9] X. Xu, W.L. Daniel, W. Wei, C.A. Mirkin, *Small* 6 (2010) 623–626.
- [10] S.J. Hurst, M.S. Han, A.K. Lytton-Jean, C.A. Mirkin, *Anal. Chem.* 79 (2007) 7201–7205.
- [11] J.S. Lee, P.A. Ulmann, M.S. Han, C.A. Mirkin, *Nano Lett.* 8 (2008) 529–533.
- [12] G. Liu, R. Lao, L. Xu, Q. Xu, L. Li, M. Zhang, S. Song, C. Fan, *Biosens. Bioelectron.* 42 (2013) 516–521.
- [13] H. Xu, M.Y. Sha, E.Y. Wong, J. Uphoff, Y. Xu, J.A. Treadway, A. Truong, E. O'Brien, S. Asquith, M. Stubbins, N.K. Spurr, E.H. Lai, W. Mahoney, *Nucl. Acids Res.* 31 (2003) e43.
- [14] J. Zheng, M. Moorhead, L. Weng, F. Siddiqui, V.E. Carlton, J.S. Ireland, L. Lee, J. Peterson, J. Wilkins, S. Lin, Z. Kan, S. Seshagiri, R.W. Davis, M. Faham, *Proc. Natl. Acad. Sci. USA* 106 (2009) 6712–6717.
- [15] S.H. Han, L.S. Park, J.-S. Lee, *J. Mater. Chem.* 22 (2012) 20223–20231.
- [16] Y.C. Cao, R. Jin, C.S. Thaxton, C.A. Mirkin, *Talanta* 67 (2005) 449–455.
- [17] G.D. Huy, M. Zhang, P. Zuo, B.C. Ye, *Analyst* 136 (2011) 3289–3294.
- [18] L.J. Ou, P.Y. Jin, X. Chu, J.H. Jiang, R.Q. Yu, *Anal. Chem.* 82 (2010) 6015–6024.
- [19] R.A. Reynolds, C.A. Mirkin, R.L. Letsinger, *J. Am. Chem. Soc.* 122 (2000) 3795–3796.
- [20] Y. Liu, Z. Wu, G. Zhou, Z. He, X. Zhou, A. Shen, J. Hu, *Chem. Commun.* 48 (2012) 3164–3166.
- [21] L. Lu, H. Wang, Y. Zhou, S. Xi, H. Zhang, J. Hu, B. Zhao, *Chem. Commun.* (2) (2002) 144–145.
- [22] S.J. Hurst, A.K.R. Lytton-Jean, C.A. Mirkin, *Anal. Chem.* 78 (2006) 8313–8318.
- [23] M.W. Berry, M. Browne, A.N. Langville, V.P. Pauca, R.J. Plemmons, *Comput. Stat. Data Anal.* 52 (2007) 155–173.
- [24] W. Xie, C. Herrmann, K. Kompe, M. Haase, S. Schlucker, *J. Am. Chem. Soc.* 133 (2011) 19302–19305.
- [25] R. Jin, G. Wu, Z. Li, C.A. Mirkin, G.C. Schatz, *J. Am. Chem. Soc.* 125 (2003) 1643–1654.
- [26] L.M. Zanolli, R. D'Agata, G. Spoto, *Anal. Bioanal. Chem.* 402 (2012) 1759–1771.
- [27] A.W. Peterson, R.J. Heaton, R.M. Georgiadis, *Nucl. Acids Res.* 29 (2001) 5163–5168.
- [28] J.E. Smith, D.K. Griffin, J.K. Leny, J.A. Hagen, J.L. Chávez, N. Kelley-Loughnane, *Talanta* 121 (2014) 247–255.